

DESIGN OF PRACTICAL PULSE COMPRESSION WAVEFORMS FOR POLARIMETRIC PHASED ARRAY RADAR

David Schwartzman* and Sebastián M. Torres

Cooperative Institute for Mesoscale Meteorological Studies, University of Oklahoma, and NOAA/OAR/National Severe Storms Laboratory, Norman, Oklahoma

1. INTRODUCTION

Active Phased Array Radar (PAR) systems use solid-state transmit-receive (TR) modules to produce a collimated electromagnetic beam. Altogether, these relatively low-powered TR modules result in a peak transmit power that is typically lower than with conventional high-power amplifiers (e.g., klystrons or magnetrons) used in radars with parabolic-reflector antennas. This results in a lower PAR sensitivity when using the same pulse envelope as a conventional radar system. That is, the sensitivity of conventional radars that use a single high-power transmitter may be difficult to achieve with a PAR system without employing advanced techniques.

Pulse compression provides increased sensitivity without affecting the range resolution (Barton, 1975). Initially developed for point targets, pulse compression consists of transmitting a long pulse to increase the average power and later compressing it to the desired range resolution at the receiver using a matched filter. More recently, pulse compression has been implemented on ground-based weather radars (e.g., O'Hara and Bech 2007, Kurdzo et al. 2014, Orzel and Frasier 2018), proving to be an effective technique to improve sensitivity when dealing with distributed scatterers. However, the transmission of long pulses may spread power over a large number of scatterers along range, which can contaminate samples from a range location with returns from adjacent locations.

The range weighting function (RWF) weighs the returned powers from scatterers in range. It is defined as the convolution of the receiver impulse response $h(l\Delta t)$ and the transmitted waveform $e(l\Delta t)$ (Doviak and Zrnić, 1993),

$$W(l\Delta t) = e(l\Delta t) \otimes h(l\Delta t) = \sum_{n=1}^{N_w} e(n\Delta t) h(l\Delta t - n\Delta t), \quad (1)$$

* Corresponding author address: David Schwartzman, 120 David L. Boren Blvd, Room 4427, Norman, OK, 73072. E-mail: David.Schwartzman@noaa.gov.

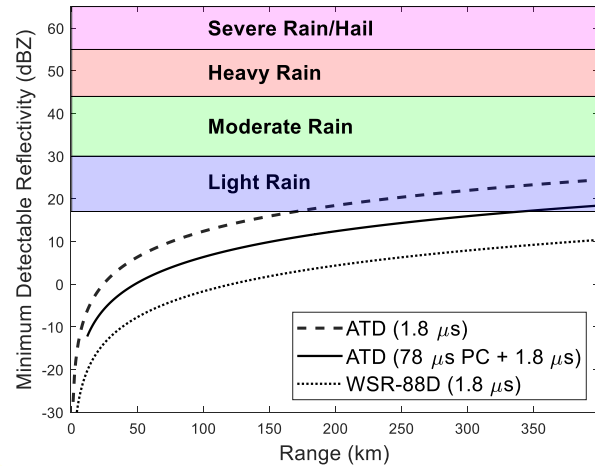


Fig. 1. Minimum detectable reflectivity as a function of range. These curves illustrate the sensitivity of the ATD system using pulse-compression waveforms.

where Δt is the temporal sampling spacing, l is the range-sample index, and N_w is the number of waveform samples. The RWF from pulse-compression waveforms exhibits range sidelobes that extend beyond the range-gate spacing, and may result in contaminated measurements. Even if a pulse-compression waveform is theoretically designed to have acceptable RWF sidelobe levels, practical effects introduced by the system may increase these sidelobe levels beyond acceptable limits. Thus, to meet strict range resolution requirements and attain desired performance, practical system effects should be considered in the design process.

The Advanced Technology Demonstrator (ATD) is an active S-band planar dual-polarization PAR that is funded through a joint collaboration of the National Oceanic and Atmospheric Administration (NOAA) and the Federal Aviation Administration (FAA). It is being developed by the National Severe Storms Laboratory (NSSL), the Cooperative Institute for Mesoscale Meteorological Studies (CIMMS) at the University of Oklahoma, MIT Lincoln Laboratory, and General Dynamics Mission Systems (Stailey and Hondl, 2016, Conway et al. 2018, Torres and Hondl 2018). This proof-of-



Fig. 2. Reflectivity fields from the 01 May 2019 weather event at ~195825 UTC collected with (left) ATD using a short waveform, (center) ATD using a pulse-compression waveform, and (right) operational KTLX WSR-88D.

concept system makes use of pulse compression waveforms to meet sensitivity and range-resolution requirements. Each of the 4,864 antenna elements radiates 6 W of power per polarization for a peak power of ~29.2 kW, which is much lower than the 750 kW of the Weather Surveillance Radar – 1988 Doppler (WSR-88D). Fig.1 illustrates the sensitivity improvement of the ATD when using a 78- μ s pulse-compression waveform over using a short 1.8 μ s pulse. Fig. 2 illustrates this sensitivity improvement on fields of reflectivity estimates, where data from the operational KTLX (Twin Lakes, OK) WSR-88D radar is shown for reference.

In this paper, we take a preliminary look at distortions introduced by the ATD on pulse compression waveforms, we provide design considerations to address practical system effects, and we illustrate the performance of practical waveforms with real data. Results of this work are expected to lead to the design of practical pulse-compression waveforms for the ATD that are able to meet demanding range-resolution requirements by incorporating system effects in the design process.

2. BACKGROUND

A requirement-driven waveform-design optimization framework was developed to produce pulse-compression waveforms to meet sensitivity and range-resolution requirements on the ATD (Torres et al. 2017). Range oversampling (RO) and averaging (Torres 2001) is used in conjunction with pulse compression to reduce the variance of radar-variable estimates. The objective function to minimize is composed of three terms: transmission bandwidth, a reduction factor for the variance of estimates, and the *integrated contamination* (IC).

The IC represents the power of the RWF that exceeds the requirements, as determined by a range envelope defined in dB as

$$IC = 10 \log_{10} \left\{ \frac{1}{2N_w} \sum_{n=-N_w}^{N_w} \frac{\max[W(n\Delta r), E(n\Delta r)]}{E(n\Delta r)} \right\}, \quad (2)$$

where W is the range weighting function defined in (1), E is the range envelope function, and Δr is the range sampling spacing ($c\Delta t/2$). An ideal RWF that meets the range-envelope requirement results in an IC of 0 dB. The Signal Processing And Radar Characteristics (SPARC, Schwartzman and Curtis 2019) simulator was used to simulate the performance of the ATD system including the effects of these pulse-compression waveforms. Simulations illustrate that the contamination introduced by the range sidelobes of the designed waveform is negligible. Nevertheless, these simulations assumed ideal hardware performance and did not account for waveform distortions on the transmit and receive processing paths.

Prior to the installation of the ATD in the National Weather Radar Testbed in Norman, OK, a few pulse compression waveforms were measured in the MIT-Lincoln Laboratory near-field chamber during April 2018. The transmit waveforms sampled at 100 MSPS were loaded in the digital exciter, transmitted with the full array, received with a near-field probe, and looped back into the radar receiver. Time-series data were digitized and recorded at 8 MSPS. Fig. 3 illustrates the designed and measured waveforms in panels (a) and (b), respectively, and their corresponding RWF in panel (c). The 78- μ s pulse-compression waveform sweeps a bandwidth of 6 MHz for a time-bandwidth product of 468. Note that the sidelobe

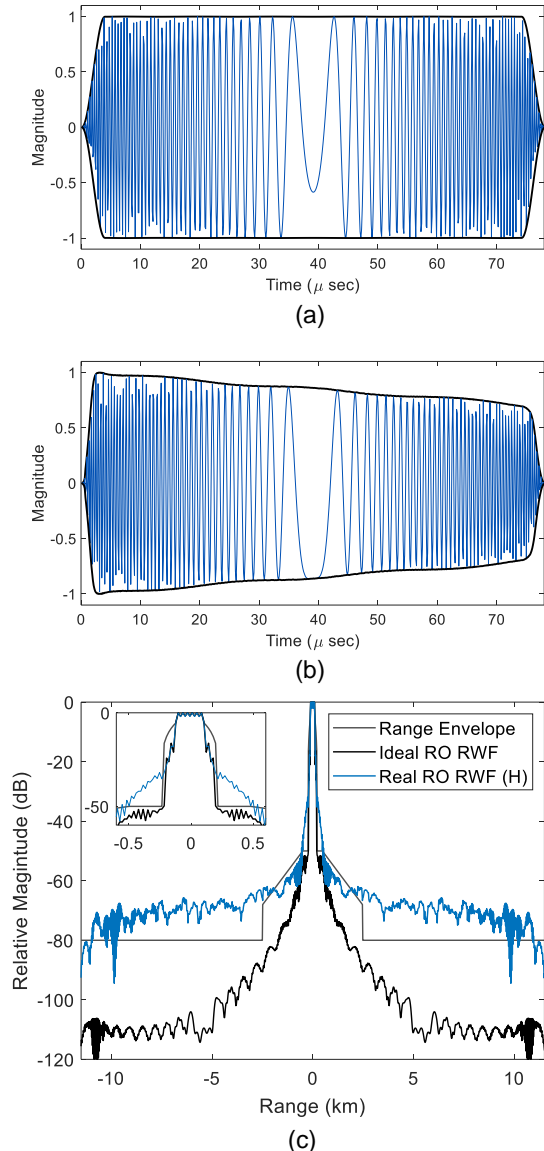


Fig. 3 (a) Designed waveform (b) measured waveform (c) RWF of the designed (black) and measured (blue) waveforms. Note that the sidelobe contamination of the measured RWF exceeds the range envelope.

contamination of the measured RWF exceeds the range envelope with an IC of 2.26 dB. This range-sidelobe contamination may significantly bias radar-variable estimates in the presence of strong reflectivity gradients. Furthermore, the waveform measurements obtained for each polarization revealed that the difference in magnitude and phase distortions on the horizontal (H) and vertical (V) polarizations could introduce additional biases on polarimetric-variable estimates. These distortions should be taken into account to produce RWFs on the H and V channels that meet both

range-sidelobe and polarimetric-variable bias requirements (e.g., Z_{DR} bias < 0.1 dB).

In the following section, we provide considerations for the design of practical pulse-compression waveforms.

3. OPTIONS FOR PRACTICAL DESIGN OF PULSE COMPRESSION WAVEFORMS

Typically, system effects on pulse compression waveforms are addressed by pre-distorting in magnitude and phase (herein called *full pre-distortion*) or by using mismatched receiver filters. Full pre-distortion may result in better performance in terms of RWF sidelobe levels, but it comes at a price of reduced sensitivity. The use of a mismatched filter may not be very effective compared to full pre-distortion due to the down-sampled nature of the received data. Furthermore, given that TR modules have a non-linear response and are usually operated at their compression point, a perfect full pre-distortion may be difficult to achieve in general.

Considering these tradeoffs, we propose a third option: the design of a phase-only pre-distorted waveform on transmit and the use of a mismatched filter on receive. Notice that system sensitivity is not compromised with this approach, and the required range-sidelobe performance can be achieved. We describe and illustrate the tradeoffs of these options in the following sub-sections.

3.1 Option 1: Full pre-distortion

Full pre-distortion could be a desirable option if the practical (or radiated) waveform were very similar to the ideal (or designed) one. In this case, since the waveform impinging on the scatterers is similar to the designed waveform, it results in nearly ideal RWF performance on receive. However, there is a sensitivity loss associated with full pre-distortion because the distortion correction that includes compensation for amplitude droop must be scaled to the transmitter peak power.

A full pre-distortion technique has been demonstrated on the PX-1000 dual-polarization weather radar developed by the Advanced Radar Research Center (Kurdzo 2014b). This radar has solid-state transmitters for each polarization, which inject the H and V waveforms into the ports of the feed to a parabolic-reflector antenna.

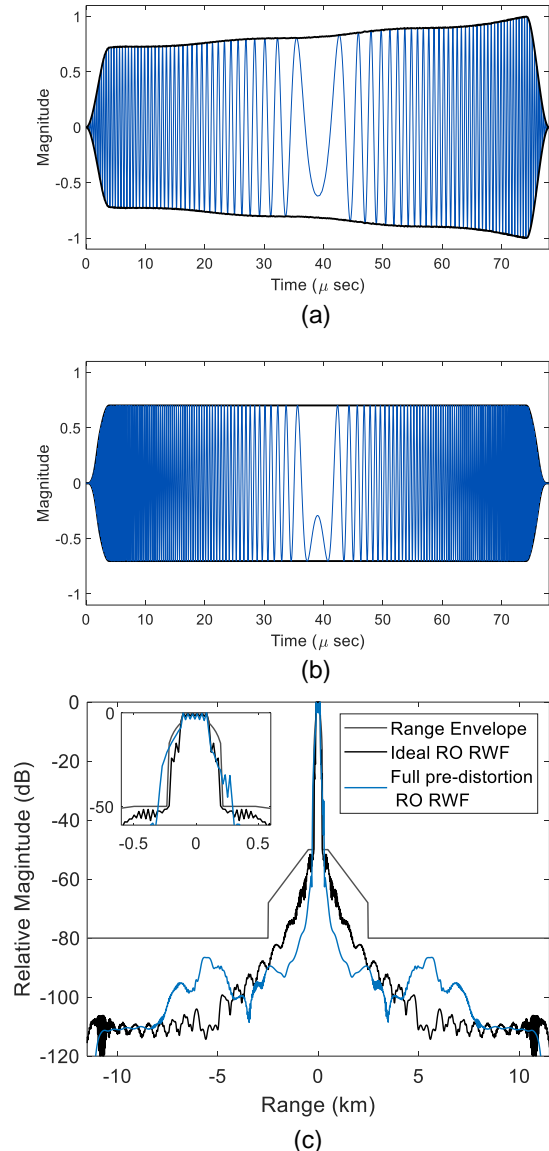


Fig. 4 (a) Full pre-distortion waveform that compensates for magnitude and phase distortions introduced by the ATD system (b) Radiated waveform modeled using the measured and pre-distorted waveforms (c) Full pre-distortion RWF.

For the ATD, we used the 78- μ s waveform shown in Fig. 3(b) (up-sampled to 100 MSPS) and produced an optimized full pre-distortion waveform that minimizes the IC of the RWF. This is presented in Fig. 4(a), where the peak magnitude is normalized to 1. Fig. 4(b) shows the waveform that would be radiated by the system (assuming a linear behavior of the TR modules) when injecting the designed full pre-distortion waveform. There is a 3.1 dB sensitivity loss incurred when using this waveform, but the IC of the corresponding RWF is 0.46 dB (i.e., mostly below the range envelope).

This is an attractive option to account for system-induced distortions provided that TR module non-linearity can be modeled. Nevertheless, with sensitivity improvement being the driver for the use of pulse compression, the sensitivity loss incurred by this method makes this option less appealing. In the following section, we discuss the use of a mismatched filter on the receiver as a means to compensate for system distortions without compromising system sensitivity.

3.2 Option 2: Mismatched receiver filter

It is well known that the receiver matched filter maximizes the output signal-to-noise ratio (SNR). Nevertheless, mismatched filters are typically used to reduce sidelobe contamination at the price of an SNR loss. Given that the range sidelobes from practical RWFs may exceed desired requirements, the use of mismatched filters may be a feasible alternative.

This technique is applied at the receiver, and there is no loss of sensitivity on transmit. However, assuming that no compensation is applied on transmit, decimated data received at the input of the filter are distorted by the system. The performance of the filter in terms of reducing the range sidelobes of the RWF depends on the digital receiver sampling rate at the input of the filter. Naturally, higher sampling rates result in better filter performance.

The exciter on the ATD system generates RF waveforms from a digital waveform definition at a rate of 100 MSPS, and its digital receiver produces digitized signals at a rate of 8 MSPS. The waveform shown in Fig 3(b) was used in the optimization framework as the transmit waveform (at 100 MSPS), and a mismatched receiver filter was designed at 8 MSPS with the objective of minimizing the IC of the RWF. The resulting mismatched filter and its corresponding RWF are shown in Fig 5. While the performance of this RWF is lower than that of the full pre-distortion technique, it is close to meeting the range-sidelobe requirements imposed by the envelope. The use of a phase-only pre-distortion technique coupled with a mismatched filter on receive may provide a way to achieve these demanding requirements.

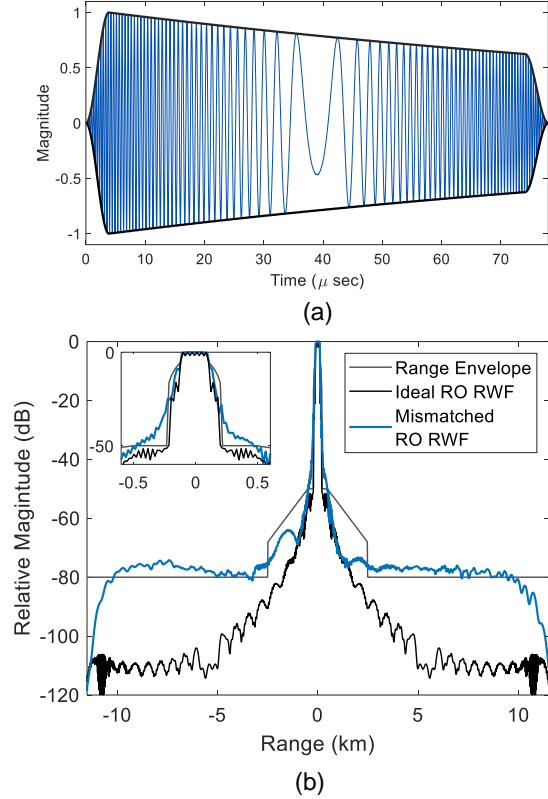


Fig. 5 (a) Mismatched waveform that compensates for magnitude and phase distortions introduced by the ATD system (b) Mismatched RWF.

3.3 Option 3: Phase pre-distortion and mismatched filter

To maximize sensitivity on transmit, a practical waveform design option is to pre-distort only the phase of the transmit waveform and use a mismatched receiver filter. While the performance (in terms of range-sidelobe reduction) of this technique may be lower than that of the full pre-distortion, it could provide a pair of waveforms (transmit and receive) with a resulting RWF that meets requirements.

For weather radars detecting precipitation echoes, system sensitivity is an important parameter, and as was mentioned before, this is especially important for PARs with relatively low-powered TR modules. Therefore, this technique is preferred over the previous ones, as long as performance meets the imposed range-sidelobe requirements. In addition, given that this technique does not require to pre-distort the waveform magnitude, distortion modeling could be easier. We show the real RWF for this option in Section 5.

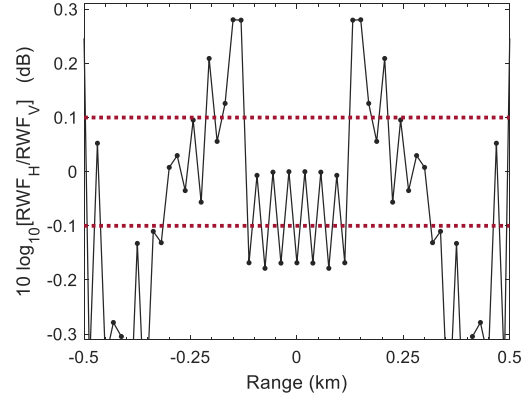


Fig. 6. Ratio of the H and V RWFs from the 78 μ s ATD waveform measured at the MIT-Lincoln Laboratory anechoic chamber.

4. POLARIMETRIC PAR CONSIDERATIONS

For polarimetric radars, the matching of the H and V RWF should also be considered in the design of practical waveforms. That is, to meet demanding data-quality requirements (e.g., Z_{DR} bias < 0.1 dB), the RWFs for H and V should be relatively well matched near the center of the resolution volume.

We illustrate these potential differences in Fig. 6 by taking the ratio of the H and V RWFs from the 78- μ s ATD waveform measured in an anechoic chamber. The dotted lines represent the required 0.1 dB maximum bias for differential reflectivity estimates. While some of the samples are within the requirement, several others close to the center of the resolution volume are not. These measurements serve to illustrate the importance of polarimetric RWF matching to meet data-quality requirements.

One way to account for these differences in the practical waveform design is to introduce an additional penalty function in the optimization. The *Polarization Mismatch Contamination (PMC)* is defined here as the power difference between the H and V RWFs weighted by the geometric mean of these RWFs,

$$PMC = 10 \log_{10} \left\{ \frac{1}{2N_w} \sum_{n=-N_w}^{N_w} \frac{|RWF_H(n\Delta r)|}{|RWF_V(n\Delta r)|} \dots \sqrt{RWF_H(n\Delta r)RWF_V(n\Delta r)} \right\}, \quad (3)$$

where the geometric mean is introduced to weigh the relative difference by an equivalent absolute RWF. A waveform optimization framework can be posed by jointly minimizing a combination of the IC and PMC penalties in equations (2) and (3).

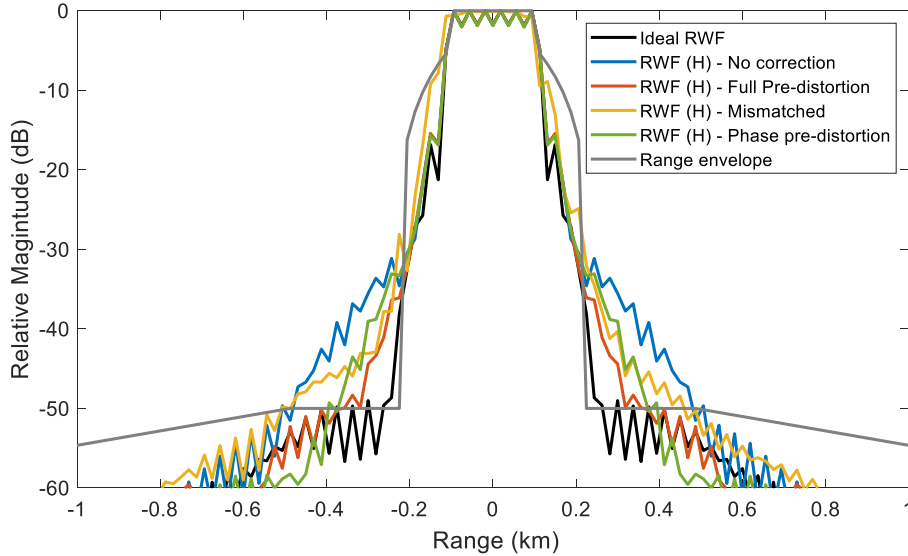


Fig. 7. RWF performance comparison. All except the ideal RWF were measured with the ATD system.

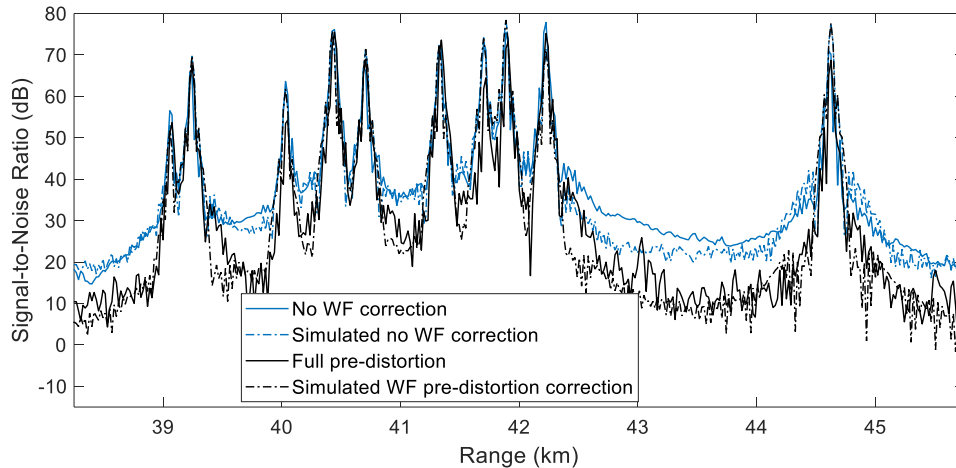


Fig. 8. Simulated and measured returns from point targets in the Oklahoma City metro area using the RWFs shown in Fig. 7.

5. PERFORMANCE OF PRACTICAL WAVEFORMS ON THE ATD

Practical pulse-compression waveforms were designed using the three options presented in Section 3 and loaded on the ATD system. Using real point targets (i.e., radio towers), a train of 64 pulses were transmitted with each of the waveforms, and the received IQ data were archived for analysis. The RWFs obtained are presented in Fig. 7, where the ideal RWF (solid black) is included for reference. It is noted that the full pre-distortion and phase pre-distortion waveforms have similar overall performance. The full pre-distortion waveform was used to collect point target-data first and weather data later.

For the point-target collection, the radar was pointed towards the Oklahoma City metro area, where several radio and TV stations are located. In addition, the range of each tower was calculated using global coordinates and their returns were simulated assuming ideal point-target conditions. This was used to validate the measurements and the expected performance of these waveforms in preparation for weather data collection. These simulations and measurements are presented in Fig. 8. Notice that the full pre-distortion waveform significantly outperforms its uncorrected counterpart, and that the simulated point-target returns are in good agreement with the measured ones. After verifying the performance of the waveforms using non-meteorological targets, the

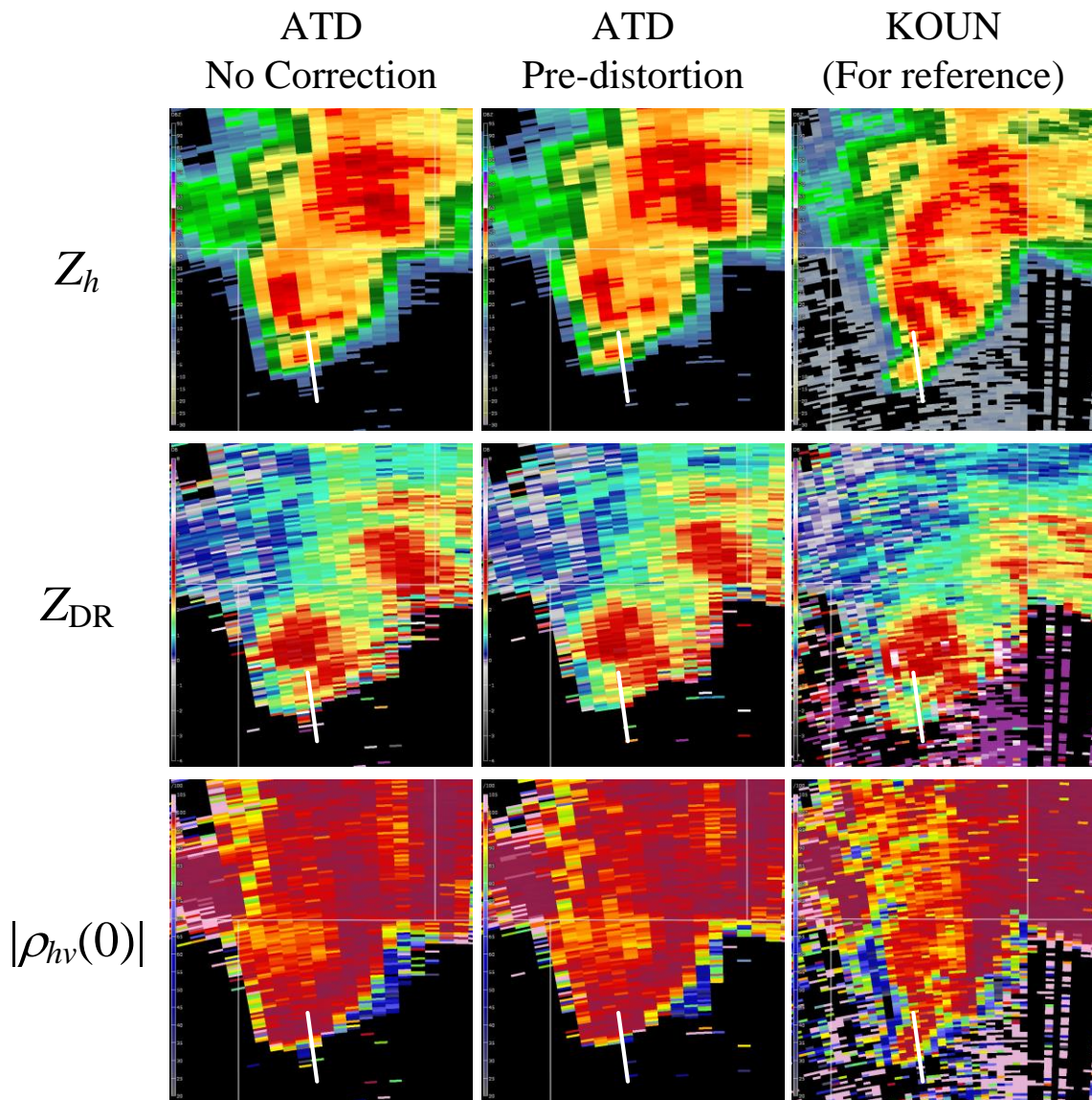


Fig. 9. Data collected with the ATD and the KOUN (WSR-88D in Norman, OK) radars on 20 May 2019 at ~ 210115 Z and ~ 210302 Z, respectively. The left and center columns show ATD data collected with the uncorrected and full pre-distortion waveforms, and the right column shows KOUN data for reference. The white line indicates a reflectivity gradient where range-sidelobe contamination is present and more apparent on the uncorrected waveform data.

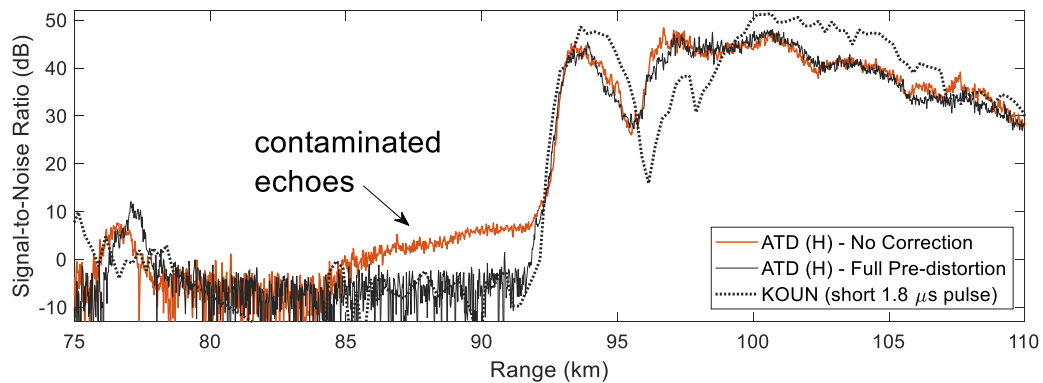


Fig. 10. SNR profiles of the waveforms in Fig. 9, along the white radial line. This confirms the hypothesis that range-sidelobe contamination is spreading the reflectivity gradient.

ATD was used to collect weather data during the severe weather event on 20 May 2019 in Oklahoma City, OK. The collected data were processed using several signal processing techniques including radial-by-radial noise estimation (Ivić et al. 2013), ground clutter filtering (Torres and Warde 2014), and range oversampling and averaging (Torres and Ivić 2005). Copolar beamsteering biases introduced by the system were mitigated by applying corrections derived from beam-peak measurements (Ivić 2018, Fulton et al. 2018, Ivić and Schwartzman 2019) to produce reasonable polarimetric-variable estimates. Radar-variable estimates computed using data from the uncorrected waveform and the full pre-distortion waveform are shown in Fig. 9. Data from the WSR-88D KOUN radar (i.e., no pulse compression) is shown for reference on the third column. The rows from top to bottom show fields of reflectivity (Z_h), Z_{DR} , and copolar correlation coefficient ($|\rho_{hv}(0)|$). The white line indicates a region where strong radial reflectivity gradients are present. It is apparent from these estimates that there is range-sidelobe contamination spreading from these gradients on data from the uncorrected waveform. That is, there are several resolution volumes with weak Z_h echoes extending south of the strong gradients, coupled with high Z_{DR} and very low $|\rho_{hv}(0)|$ estimates. In contrast, the data from the full pre-distortion waveform does not exhibit these echoes in any of the fields in that region. To confirm that these echoes are coming from range sidelobes, the SNRs from the H polarization along that radial are plotted on Fig. 10. It is evident from these plots that the weak echoes on the uncorrected waveform data are a consequence of relatively poor waveform performance.

6. SUMMARY

In this paper, we provide considerations for the design of practical pulse-compression waveforms on polarimetric PAR systems. Pulse compression can always enhance the detection of radar signals provided that range sidelobes are well constrained. However, practical system distortions have to be accounted for in the design process to effectively achieve the desired performance.

We discussed three options for designing practical pulse-compression waveforms: full pre-distortion, mismatched filter, and phase pre-distortion with mismatched filter. The performance

of these techniques has to be thoroughly quantified to fully understand the tradeoffs associated with each one. While this paper only presents an intuitive analysis of these tradeoffs, a more in-depth and systematic study is ongoing.

We also introduced an additional consideration for polarimetric PARs using pulse-compression waveform. Minimizing the PMC is fundamental to achieve polarimetric data quality requirements. Finally, we illustrated the full pre-distortion technique described using the ATD system. First, data from a set of point targets were collected using both uncorrected and full pre-distortion waveforms. These showing good agreement with simulated targets. Then, weather data were collected using both waveforms during a severe weather event on which strong gradients were observed.

This paper serves as a motivation to expand the analysis on practical design of pulse-compression waveforms on the ATD. In the near future, the full calibration infrastructure currently being integrated to the system will be used to more accurately and completely quantify the performance of different correction techniques. In addition to the findings presented in this paper, we are also planning to characterize the system distortions as a function of transmission bandwidth and pulse width. By incorporating practical system effects into the design of pulse-compression waveforms, we hope to produce weather data with quality that meets the NWS mission requirements.

ACKNOWLEDGMENT

We would like to thank Dr. Antone Kusmanoff (University of Oklahoma, JHLP) and Jami Boettcher (University of Oklahoma, CIMMS) for useful comments that improved this paper. We would also like to extend our appreciation to the entire ATD team. Special thanks go to Christopher Schwarz (University of Oklahoma, CIMMS), Daniel Wasielewski (NOAA-NSSL), Rafael Mendoza (NOAA-NSSL), John Murdock (GD-MS), and Alexander Morris (MIT-LL) for their support configuring and operating the ATD.

This conference paper was prepared with funding provided by NOAA/Office of Oceanic and Atmospheric Research under NOAA-University of Oklahoma Cooperative Agreement #NA16OAR4320115, U.S. Department of Commerce.

REFERENCES

- Barton, D. K., 1975: *Radars. Volume 3 – Pulse Compression*, Dedham MA, Artech House, Inc.
- Conway, M. D., D. Du Russel, A. Morris, and C. Parry, 2018: Multifunction phased array radar advanced technology demonstrator nearfield test results. *Proc. of the IEEE*, doi: <https://doi.org/10.1109/RADAR.2018.8378771>
- Doviak, R. J., and D. S. Zrnić, 1993: *Doppler Radar and Weather Observations*. Academic Press, 562 pp.
- Fulton, C., J. Salazar, D. Zrnić, D. Mirković, I. Ivić, and D. Doviak, 2018: Polarimetric Phased Array Calibration for Large-Scale Multi-Mission Radar Applications, *IEEE Radar Conference (RadarConf18)* doi: <https://doi.org/10.1109/RADAR.2018.8378746>
- Ivić, I. R., C. Curtis, and S.M. Torres, 2013: Radial-Based Noise Power Estimation for Weather Radars. *J. Atmos. Oceanic Technol.*, **30**, 2737–2753, <https://doi.org/10.1175/JTECH-D-13-00008.1>
- Ivić, I. R., 2018: Options for Polarimetric Variable Measurements on the MPAR Advanced Technology Demonstrator, *IEEE Radar Conference (RadarConf18)*, doi: <https://doi.org/10.1109/RADAR.2018.8378544>.
- Ivić, I. R., and D. Schwartzman 2019: A first look at the ATD data corrections. Preprints, *39th International Conference on Radar Meteorology*, Nara, Japan. Amer. Meteor. Soc., Paper 2-06.
- Kurdzo, J. M., B. L. Cheong, R. Palmer, G. Zhang, and J. Meier, 2014a: A pulse compression waveform for improved-sensitivity weather radar observations. *J. Atmos. Oceanic Technol.*, **31**, 2713–2731, doi: <https://doi.org/10.1175/JTECH-D-13-00021.1>.
- Kurdzo, J.M., B. L. Cheong, R. Palmer and G. Zhang, 2014b: Optimized NLFM pulse compression waveforms for high-sensitivity radar observations. *International Radar Conference*, Lille, France. doi: <https://doi.org/10.1109/RADAR.2014.7060249>
- O’Hora, F., and J. Bech, 2007: Improving weather radar observations using pulse-compression techniques. *Meteor. Appl.*, **14**, 389–401, doi: <https://doi.org/10.1002/met.38>.
- Orzel, K.A., and S. J. Frasier, "Weather Observation by an Electronically Scanned Dual-Polarization Phase-Tilt Radar," in *IEEE Transactions on Geoscience and Remote Sensing*, vol. 56, no. 5, pp. 2722-2734, May 2018. doi: <https://doi.org/10.1109/TGRS.2017.2782480>
- Stailey, J. E., and K. D. Hondl, 2016: Multifunction phased array radar for aircraft and weather surveillance. *Proc. IEEE*, **104**, 649–659, doi: <https://doi.org/10.1109/JPROC.2015.2491179>.
- Schwartzman, D.; and C.D. Curtis, 2019: Signal processing and radar characteristics (SPARC) simulator: A flexible dual-polarization weather-radar signal simulation framework based on preexisting radar-variable data. *IEEE J. Sel. Top. Appl. Earth Observ.*, **12**, 135–150, doi: <https://doi.org/10.1109/JSTARS.2018.2885614>
- Torres, S., 2001: Estimation of Doppler and polarimetric variables for weather radars. Ph.D. dissertation, University of Oklahoma, 158 pp.
- Torres, S. and I. R. Ivić, 2005: Demonstration of range oversampling techniques on the WSR-88D. Preprints, *32nd International Conference on Radar Meteorology*, Albuquerque, NM, Amer. Meteor. Soc., Paper 4R.5.
- Torres, S.M. and D.A. Warde, 2014: Ground Clutter Mitigation for Weather Radars Using the Autocorrelation Spectral Density. *J. Atmos. Oceanic Technol.*, **31**, 2049–2066, <https://doi.org/10.1175/JTECH-D-13-00117.1>.
- Torres, S.M., C.D. Curtis, and D. Schwartzman, 2017: Requirement-Driven Design of Pulse Compression Waveforms for Weather Radars. *J. Atmos. Oceanic Technol.*, **34**, 1351–1369, <https://doi.org/10.1175/JTECH-D-16-0231.1>
- Torres, S. and K. Hondl, 2018: The Advanced Technology Demonstrator at the National Severe Storms Laboratory. 10th European Conf. on Radar Meteor. and Hydrology (ERAD), Ede, Netherlands, KNMI and Wageningen University, Paper 178.